Experimental investigation on the bond-slip law of deformed bars in concrete

Experimental Investigation on the Bond-Slip Law of Deformed Bars in Concrete

Recherche expérimentale sur la relation adhérence-glissement des barres nervurées dans le béton

Versuche zum Verbundgesetz von Rippenstählen in Beton

EZIO GIURIANI
Ass. Professor
Institute of Structural Engineering (ISTC), Politecnico di Milano
Milan, Italy

SUMMARY
The paper shows the results of a series of tests aimed at the analysis of the reinforcement-concrete bond, for very small relative displacements (under 0.1 mm). Several pull-out tests were carried out on cubic specimens, having a single bar with only two ribs embedded in the concrete.
The bond stiffness was analysed for different positions of the ribs, for cyclic loads with or without sign reversal. The effects of the concrete hardness at the interface with the reinforcement are discussed and the bond mechanism is examined in terms of microcracking and concrete crushing.

RÉSUMÉ
Dans cette étude on montre les résultats d'une série d'essais expérimentaux pour la détermination de la loi d'adhérence acier-béton, pour des déplacements relativement petits (inférieurs à 0,1 mm).
Plusieures épreuves de pull-out ont été faites sur des cubes d'essai avec une barre ayant seulement deux nervures faisant prise dans le béton.
On a étudié l'influence sur l'adhérence des diverses positions des nervures dans les cubes pour des charges répétées avec ou sans inversion de signe.
On analyse l'influence de la résistance du béton en contact avec l'acier et on discute le mécanisme de microfissuration et d'écrasement près des nervures.

ZUSAMMENFASSUNG
Der Beitrag zeigt die Ergebnisse einer Versuchsreihe zum Verbundverhalten von Rippenstählen im Beton mit sehr kleinen Relativverschiebungen (< 0,1 mm). Mehrere Ausziehversuche wurden an Würfeln ausgeführt, in die Einzelstäbe mit zwei Rippen einbetoniert waren.
Die Verbundsteifigkeit wurde untersucht für verschiedene Rippenlagen und für Wechselbelastung und Schwingbelastung. Der Einfluss der Betonhärte in Stabnähe auf des Verbundverhalten wurde mithilfe von Mikrorissbildung und Betondruckversagen erläutert.

1. INTRODUCTION

The bond between reinforcing bars and concrete is a very important factor not only in anchorage but also in cracking.

In /1/ it was shown that the deformations in r.c.beams,at the beginningof the second stage (when the main cracks begin and extend progressively), are largely conditioned by the bond which affects also the so-called tension stiffening in the advanced second stage. According to the model proposed in /1/, (*) and with reference to beams in bending, in the first stage the micro-cracks begin to propagate starting from the extreme tensile fiber until reaching the reinforcement. Their progressive opening up is compatible with the elastic strains in the concrete between the microcracks, and there is no slip at the interface between reinforcement and concrete (chemical adhesion phase).

After this phase, the chemical adhesion is progressively destroyed, starting from the flexural cracks, and in this same zone the bar-to-concrete slip begins (^).

This gradual loss of chemical adhesion progresses until it involves the entire surface of the reinforcement between two main consecutive cracks (+), thus setting up different static conditions for the steel in which bond decreases in importance.

All of this justifies a thorough study of the bond-slip law, particularly for small displacements. In fact, very little work has so far been done in this field (').

2. PURPOSE OF THE RESEARCH

The researchwork, which this paper refers to, is focused on the local bond behaviour, with reference to the bond law of a single rib within the range of very small slip values.

The tests are limited to one type of deformed bar with a nominal diameter of 14 mm (Fig.2) (") and consist of load cycles, with maximum slip less than one tenth of a millimeter; after the last cycle (generally the third cycle), the loads were monotonically increased up to failure with much larger displace-

---

(*) With a maximum amplitude of only some thousandths of a millimeter, and so visible only through a microscope.

(^) The bar length, over which the slip occurs, plays an important role also with reference to other problems, such as for example fracture mechanics of reinforced concrete and shear transmission through aggregate interlock.

(+) The main cracks (which generally develop from micro-cracks) form and advance progressively, all at the same time, up to the end of stage II (as shown by many tests, including those of Leonhardt in Stuttgart).

(') Even the most recent literature, though abounding in experimental and theoretical work ón bond, is generally directed towards large strains and displacements.

(") The kind of reinforcing bar chosen for the tests,with slanting ribs (see Fig.2) is becoming more and more widely used in practice.

ments. [*]

During the tests useful information was also gathered on various phenomena that occur in the vicinity of the ribs. Though these phenomena have already been discussed by other authors, their effect on small relative displacements is still uncertain.

As already shown by Goto /2/ (Fig.1), radial micro-cracks form around each rib immediately after the formation of the principal cracks. It has also been shown in /3/, that as slip increases, the high bearing stresses acting on the rib faces provoke local crushing in the concrete, with resulting deformations of a permanent nature. As to bond, the experimental work by Rehm /3/ is particularly valuable, since it was the first and so far still the most significant on the local bond-slip law. For his pull out tests he used a special bar with a single rib placed in the center of a concrete cube (20 cm per side) [^]. Rehm was mostly interested in comparing different types of deformed bars, and his main purpose was to determine the strengths of various rib shapes in the range of large relative displacements. He obtained a remarkable number of useful results, one of which showed the importance of the position of the reinforcement with respect to the direction of concrete casting. He noted considerable differences in the cases of a bar parallel to the casting direction or at right angles to this direction, as a result of the different porosity of the concrete surrounding the reinforcement.

In Rehm's opinion this was due to the water, which tends to rise to the surface during compaction [+]. He also noted the importance of local crushing of the concrete in contact with the reinforcement, leading to the permanent displacements already mentioned. However, since he used monotonically increasing loads, his tests can supply no certain data on the beginning of crushing [']. Furthermore, he located the bar in a central position, while often the reinforcement is located close to one of the faces of the beam, so the analysis for different positions of the rib is certainly useful ["].

(*) Beyond this value the reinforcing steel of a beam in bending generally reaches the yield point (stage III) as shown in /1/, for the usual values of crack spacing.

(^) Special lubricated sleeves around the bar, just before and after the rib, were placed to prevent the adhesion between the bar and the concrete.

(+) In the tests herein examined, the bar was always horizontal, so perpendicular to the casting direction. Furthermore, with reference to the particular rib shape, also the rib orientation is important: the lugs (sickle-shaped) were always sub-horizontal (Fig.3).

(') This problem will receive greater attention in sect. 5.

(") The deformed bars tested in the present researchwork, with sickle-shaped lugs, were not available at the time of Rehm's tests.

3. TEST PROCEDURE AND EXPERIMENTAL SET-UP

The usual pull out tests on long bars do not give suitable results for eva-
luating the local bond stress slip law. They only give the average bond
stress and the slip at the bar extremities. Specific tests are necessary to
find the local bond stress slip law, using reinforcing elements of very limi
ted length.(*)

In Fig. 2 the reinforcing element used in the test is shown. It has two ribs
on each side, and was obtained from a normal deformed bar of 14 mm in diame-
ter (core diameter 13.2 mm); its length is twice the rib spacing (16 mm).
Starting from a normal ribbed bar, the two parts adjacent to the test rib
are machined at the turning lathe, the diameter being reduced to 8 mm. The two
machined spindles are inserted in smooth aluminium sleeves, which are removed
after the concrete has hardened(^). The spindles protrude from the cube faces
(Fig.3), so that the measurement of the slip is possible at one end of the
bar, while at the other end the pull out force is applied.

In Fig. 3-a the four test positions adopted for the reinforcing element are
shown. In this way it becomes possible to analyse, within the range of small
displacements, the role played by the concrete covering, and also the local
bond stress slip law for various positions of the ribs along the bar. In
Fig. 3-b the orientation of the lugs and the direction of casting are shown(+).

The concrete test cube was glued along one face (Fig.3) to the loading set-
up in order to get as near as possible to the real conditions of the concrete
block between two flexural cracks in a beam subjected to bending (fig.3-c)(').

(*) In this way the slip will be the same at all points on the bar.

(^) The external diameter of the sleeves (14.5 mm) is the same as the exter-
    nal diameter of the lugs. The internal diameter of the sleeves is 12 mm.
    To facilitate the removal, the sleeves are covered with a film of paraf-
    fin. The cavity formed after the removal of the fore sleeve (see the
    sketch) enables the ribs to work in the same conditions as in an actual
    bar with many ribs embedded in the concrete mass.
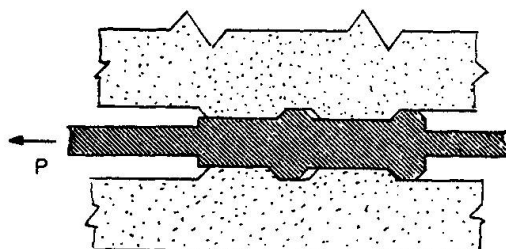
(+) Expanded polystyrene molds were used for the castings to avoid the ther
    mal gradients in the concrete during hardening.

(') In Fig. 3-a the transversal restraints of the bar: the purpose is to
    avoid misalignments of the load especially when the load is reversed.

In Fig. 3-d the layout of the instruments for the measurement of the displa
cement is shown[*].

In Figs.4,5 a picture of the test set-up is shown.Because of the length of
time (12 to 36 hours) required by each test, a loading device based on levers
and water tanks was preferred to a system of hydraulic jacks, also because
of the relatively limited value of the loads.

During the test the load was monotonically increased up to a fixed value of
the slip (7.5 hundredths of a millimeter). Next, it was reduced to zero,then
it was reversed in order to make the bar retract[^]. It was not possible to
obtain partial retractions, of pre-fixed values, because of the sudden re-
entry of the bar.

During the tests, the slip was heavily influenced by the time-rate of load
application. However, in each test, at each load step (200N), the load was
kept constant until the slip value was stable[+].

Fig.6 shows a typical time-dependent curve of the displacements: for each
load step the slip δ tends towards a stable value.

The stabilization of the slip required a considerable length of time in the
nearly horizontal branch of the τ/δ curve, with respect to the steep branch
at the lowest slip values (see Fig.7).

4. RESULTS

The geometrical characteristics of the reinforcement and the mechanical cha-
racteristics of the concrete are given in Fig.2 and tab.I. The curves refer-
ring to the bond stress and to the displacement between concrete and bar
(slip δ) are shown in Figs. 8-18.

The bond stress is defined as[']:

$$\tau_{ad} = P/(\pi d2c)$$

(*) The deflectometer applied to the bar measures the displacement of the
    two ribs embedded in concrete, while a second deflectometer measures
    any possible displacement of the cube in a point at some distance from
    the zone disturbed by the ribs.

(^) The reversal of the load to thrust the reinforcement simulates the beha
    viour of a beam in bending which, during the unloading phase, shows par-
    tial closure of the cracks, with the bars moving back.

(+) The concrete deformations were considered as stable when the time-rate
    of the slip was less than 10^{-4} mm per hour. For monotonically increasing
    loads, this criterion leads to a nearly constant slip velocity.

(') The term "bond" here is used for both chemical adhesion (with zero rela
    tive displacements) as well as for the mechanical bond with bar-to-con
    crete slip. It follows that the bond stress is actually a nominal stress
    relating the force applied to the bar to the nominal surface of the
    reinforcement (embedded in concrete).Then the bond stress takes into ac-
    count all the effects involved,such as the bearing action of the lugs,and
    the friction produced by the radial pressure of the concrete at the tops
    of the lugs.

(with P the load, d the nominal diameter of the bar and c the spacing of the ribs).

The $\tau(\delta)$ curves of each test N_i (i = 3,4,7,8) are adimensionalized, the actual values of the bond stress being divided by the value $\bar{\tau}_{N_i}$ which refers to the value 0.075 mm of the slip (the value $\bar{\tau}_{N_i}$ appears at the head of each diagram).

Fig. 8 shows the curves for test N8 with the bar in a central position. During the first cycle the load was increased up to a slip value of 0.075 mm (branch O_1 A_1 B_1 C_1). It was next decreased to zero (C_1 D_1), and then, by reversing the sign(D_1 E_1), the bar was forced to re-enter (E_1 F_1) and this occurred with virtually instantaneous slip starting at E_1[*].

The slip (at constant reverse load) stopped at a point corresponding to a residual displacement [^] (see point F_1).

The cycle was completed (branch F_1 G_1) by re-setting the load to zero. The following cycles (2 and 3) differ considerably from the first in the loading path. After a first steep short branch (G_1 H_2) the curve flattens off (H_2 K_2) with small sudden displacements in the way that is typical of friction[+].

In the branch K_2 C_2 (and also in K_3 C_3) the load was increased up to the maximum value reached in the first cycle, but the maximum relative displacement was of a higher value. The unloading paths C_2 D_2 and C_3 D_3 are practically identical with the corresponding C_1 D_1 of the first cycle.

Also the branches D_2 E_2 and D_3 E_3 are also practically identical['] with D_1E_1. In all three cases at E_1, E_2 and E_3 there is unrestrainable sudden slip up to F_1, F_2 and F_3, the latter points being very close indeed. In Figs. 9, 10, 11 the curves for the other positions of the bar (tests N 7, N4, N3) are shown. In Fig. 11 a star indicates the point at which splitting parallel to the bar first appeared (the microcrack was detected by means of a microscope). For the sake of comparison, in Fig.12 the curves for these four cases are superimposed. The comparison is limited to the first cycle and the first branch of the second cycle. The loading paths OABS show relatively modest differences["].

(*) Because of the instantaneous re-entry of the bar, the branch E_1F_1 is
    dashed. Sudden slip may be explained if one thinks that crushing has led
    to the formation of a cylindrical cavity in which the bar can move free-
    ly, apart from some unavoidable friction.

(^) This residual displacement is due to the presence of particles of aggre-
    gate in the cavity left by the lugs in the loading phase.

(+) For further details, see sect. 5.

(') The values of the reverse load needed to pass from E_2 to F_2 and from E_3
    to F_3 are a little more than half the load needed to pass from E_1 to F_1.

(") The slope of the loading path, at the origin (branch DA) is less steep
    for peripheral reinforcement, which seems reasonable.

There are also limited differences in the unloading path of the first cycles
(branch C D).The curve of test N3 is less steep as a result of a split pa
rallel to the reinforcement.

Fig.13 shows the curves obtained in test N8, with reference to cycles
4-20. The load was limited so as to get a fixed value for the relative di-
splacement (0.17 mm).

The maximum value of the ratio τ_{ad}/τ_{N8} continues to decrease for each cycle,
but with a tendency to stabilize around a value which is about two-thirds
of the initial value[*] - see the 4th cycle and the 20th cycle.

Fig.14 shows the behaviour of test specimen N8. Here the load was decreased
to zero and then increased again without any sign reversal.

In Fig. 15 the curves of the actual bond stress in the four cases examined,
are superimposed.

Although the strengths f_c of the concrete were fairly similar, as shown in
the figure, the values of τ_{Ni} [^] were very different. τ_{N8} is equal to 0.59
τ_{N4}.

The fact that the bond stresses τ_{Ni} are almost independent of the specific
strength fc of the concrete is also underlined in fig.16, where the ratio of
the bearing stresses of the lugs to concrete strength are plotted versus bar
slip[+].

The value of local bond strength depends rather on the local hardness of the
concrete adjacent to the lug, but it is difficult to evaluate['] . An examina
tion of the test cubes cut along the mean plane containing the bar axis, af-
ter the tests showed that those with lower values for local bond strength
had a more marked porosity, characterized by voids of some tenths of milli-
meters in diameter (see Fig. 17).

(*) The work dissipated in each cycle decreases as the number of cycles in-
creases. The loading and unloading paths tend to get closer for each
successive cycle, but up to a certain limit (see the modest difference
between cycles 14 and 20). Crushing of the concrete in contact with the
lugs does not seem to progress with the increase in the number of cycles.
The gradual decrease in work dissipated is perhaps due to friction bet-
ween the tops of the lugs and the concrete, which diminishes because of
the repeated scraping.

(^) As already pointed out, τ_{Ni} represents the value of local bonding corre-
sponding in the various cases tested to the relative displacement
δ = .075 mm.

(+) The concrete compressive strength was measured on prismatic specimens
(100x100x200 mm) cut out from the original cubes. The bearing stress σ_n
is defined as: $\sigma_n = P/(4a_m \cdot l_R \cdot \cos(90°-\beta))$ where a_m is the average
height, l_R the length and β the orientation of the lug (see Fig.2).

(') To the author's knowledge no data on this problem is yet available in
the literature.

Schlerometric tests were carried out on the concrete adjacent to the rein-
forcement to get some first ideas on the subject[*].

The average values from the schlerometric tests are given in table
II   . These values of course, are only partly related to the local
strength of the concrete, because of the limited section of the prod[^].
These results do make it possible to define an index of "relative hardness"
for each case, as a ratio between the hardness of the case involved and the
hardness of the test piece with central reinforcement (N8). With K_{si} to in-
dicate this relative hardness, Fig.18 shows the curves of the "reduced bond
stress" τ_{ad}/K_{si} as a function of the relative displacements. The deviation
from the mean value does not exceed $\pm$ 5%. These curves point out the impor-
tance of the local hardness of the concrete over other parameters.

Fig.19 shows the curves τ_{ad}/τ_{Ni} for large displacements (1.5 mm).

In case   N3 the appearance of the first crack (split, see point I) while
still in the range of small displacements has no appreciable effect on bond.
It is the transversal crack (II) which leads to a reduction in stiffness.
However, there is a long softening branch up to failure, which occurs at a
relative displacement of 1.7 mm[+].

5. SOME CONSIDERATIONS ON THE BOND MECHANISM

Fig.20 gives the local bond stress slip curve for test specimen N9 with
the bar close to one of the faces. As in all cases the curve shows a charac
teristic trilateral shape (OABC) with decreasing slope.

During this test, four load cycles were performed keeping the displacements
very small (less than 3/100 of a millimeter).

In the first branch of the trilateral curve (OC_1) the behaviour is practically
elastic (the first cycle has negligible hysteresis) with elastic shear in the
concrete and without any relative displacement at the bar-concrete interface
(bond is due to chemical adhesion).

After the first cycle,the load was increased up to C_2, not much beyond point A
which marks the beginning of the second branch. Then the unloading (to D_2) and
reloading up to C were carried out. The virtually elastic behaviour along
paths C_2D_2 , D_2C_2 and the residual displacement OD_2, could perhaps be explai-
ned as follows.

(*) A small test prod (tab.II) was attached to the schlerometer tip, in order
     to reach the surface of the groove left after the test cube was split
     and the bar removed. The readings were repeated about twenty times in
     different positions along the groove surface.

(^) In tab.II the concrete hardness (obtained with the reduced prod) measured
     along the groove surface and on the external surface are shown.

(+) This behaviour related to crack II is certainly less remarkable in a
     real case, with continuous reinforcement.

Once the load goes beyond a value corresponding to point A, radial micro-cracks form around the bar starting from the lug tops (Fig.21-a). When the load is reduced to zero, these micro-cracks do not completely close up. This is partly due to the friction among the aggregate particles protruding from the crack faces, but also to the wedging action of the loose particles.

After the second load cycle the load was progressively increased up to a value corresponding to point B (Fig.20), which marks the beginning of the third branch.

Once again the unloading and re-loading process was performed (C_3 D_3 and D_3 C_3), with again practically elastic behaviour and very limited hysteretic behaviour. The average slope of curves C_3 D_3 and D_3 C_3 is rather less than curves (1) and (2), because the micro-cracks propagate and spread, thus making the concrete adjacent to the lugs less rigid. Starting from C_3 the load was again increased, and crushing of the concrete in contact with the lugs began, as a result of very high bearing stresses on the lugs.

Because of concrete crushing, permanent displacements are possible (Fig.21-b): as a consequence, a cavity forms behind each lug.

Complete unloading (to D_4) was performed starting from point C_4.

During the unloading process the microcracks tend to close up almost comple-tely, but on the surfaces of the lugs the radial compressive stresses P_r con-tinue to be applied, though because of the shape$^{(*)}$ of the cavity produced during the loading process BC_4 these stresses are applied along a part of the top of the lugs.

Because of these radial stresses, the reinforcement subjected to load reversals is partially prevented from slipping back (Fig.20-d). This load, however, does help to close the micro-cracks.

When the load reached a value corresponding to point E_4 (Fig.20) a sudden slip began: this is because the equilibrium of the lug is no longer possible when the lug is pushed out of the cavity, which was produced by concrete crushing during the load process (Fig.21-d).

After the sudden slip (which occurs at constant load), the position of the lug is practically the same as the initial (no-load) position, though a slight residual slip remains, because of the loose particles detached during the loading and unloading process.

In the fourth cycle, for load levels below point K_4 (Fig.20) the bond stiff-ness is very limited, because the only force acting on the lugs is friction at the top $^{(^)}$.

(*) The nominal failure surface (Fig.21-a) makes the angle α with the defor-med surface of the concrete adjacent to the bar; because of the elastic strains, this concrete gets detached from the lateral surface of the bar, between two contiguous lugs.

(^) It is interesting to note that points E_4 (the lug leaves the crush-induced cavity) and K_4 (the lug is engaged in the crush-induced cavity) are characterized by practically the same displacements. Furthermore,the slip δ_{C1} (between E_4 and F_4, Fig.20) coincides with the length of the crush-

                                                                          ./..

Beyond point K_4, the lugs are engaged in the concrete, due to the conical surface of the cavity produced by earlier crushing; as a consequence, the bond stiffness increases (K_4H_4), because of the friction resulting from the radial pressure.

At the same time the micro-cracks again open up around the lug, so that the slope of the branch $K_4 H_4$ (Fig.20) is on average less steep than the slope of $C_4 D_4$.

At point H_4 the front face of the lug is again in contact with the crush ed concrete: it follows that the value of the bond stress in H_4 is hardly different from the value in B, which marks the beginning of concrete crushing. (Beyond H_4, further crushing occurs).

6. CONCLUSIONS

The local bond stress slip curves in the range of displacements below one tenth of a millimeter do not seem to be markedly affected by the position of the reinforcement with respect to the faces of the test cube and the amount of concrete cover.

As a consequence, the test results suggest that in a beam subjected to bending the rib-to-concrete bond is not markedly affected by the position of the rib with respect to the beam faces and to the flexural cracks.

The test results show that the considerable scattering of the values of the bond stress, for any given slip, is mostly due to the different porosity of the concrete layer immediately surrounding the bar, while the concrete compressive strength seems to be a minor factor.

Should bond stress be related to the hardness of the concrete layer in contact with the ribs (through a suitable "hardness index"), the scattering of the bond stress/slip curves will be reduced to only about 5%: the dependence of the bond strength on the hardness of the concrete along the bars seem to be so important that further tests on a larger scale ought to be carried out to confirm the above statement.

Finally, the experimental curves, obtained with cyclic loads characterized by a limited reversal, clarify the role of microcrack opening and concrete crushing with reference to bond stiffness. This role has different aspects when the load is increased (microcrack opening, possible splitting, concrete crushing) or when the load is decreased and reversed (friction at the top of the ribs, free slip to recover the cavity produced by earlier crushing).

./..
induced cavity. The slip δ_{C2} (between B and C_4) does not coincide exactly with δ_{C1}, because the crushing of the concrete occurs at the same time as the opening of the microcracks.

SYMBOLS

δ : relative displacement (slip) between the reinforcing bar and the surrounding concrete

$\tau_{ad} = P/(\pi d\, 2c)$: nominal bond stress

P   : pull-out load

d   : nominal diameter of the bar

c   : pitch of the ribs

τ_{Ni} : nominal bond stress for each test specimen at $\delta = .075$ mm

$\sigma_n = P/(4a_m l_R \cos(90-\beta^o))$: bearing stress on the ribs

a_m : average height of the ribs

l_R : length of the ribs

β^o : angle of the ribs with respect to the longitudinal axis

f_c : prismatic concrete strength of each test specimen, measured on prisms cut out from each specimen, after the pull-out test

K_{si} : relative hardness index defined as the ratio between the concrete hardness of the generic i^{th} test specimen and the hardness of the specimen with central reinforcement (N8). The hardness is measured (with a suitable sclerometric test) in the groove left by the bar in the concrete, after having cut the test specimen.

REFERENCES

/1/ Giuriani E., "Le curvature di travi in cemento armato tenso e presso-in flesse nel primo e secondo stadio" Costruzioni in Cemento Armato. Studi e Ricerche, vol. 1, 1979, Politecnico, Milano.

/2/ Goto, Y, "Cracks formed in concrete around deformed tension bars" ACI Journal, April 1971.

/3/ Rehm G., "Über die Grundlagen des Verbundes zwischen Stahl und Beton". Dafst, Heft 138, Berlin, W.Ernst u.Sohn, 1961.
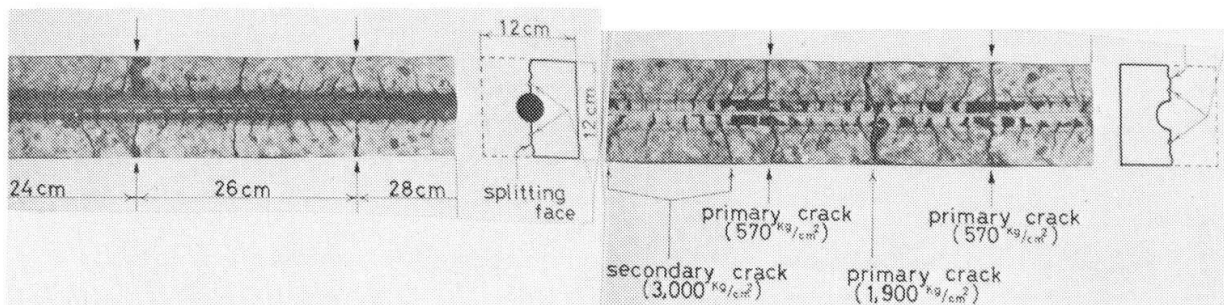
Fig. 1 - Cracking and microcracking of concrete near the ribs of a deformed bar, shown by Goto /2/

d   = 14   mm nominal diameter

ϕ = 13.95 mm diameter of the equivalent
round bar

D_K = 13.2 mm diameter of the core of the
bar

c   = 8   mm pitch of the ribs

a_m = .8   mm average height of the ribs

β = 56°   angle of the ribs

l_R = 20   mm length of the ribs

$$I_R = \frac{2\ a_m\ l_R\ \cos(90-\beta)}{\pi\ D_K\ c} = .818 \text{ bond index}$$
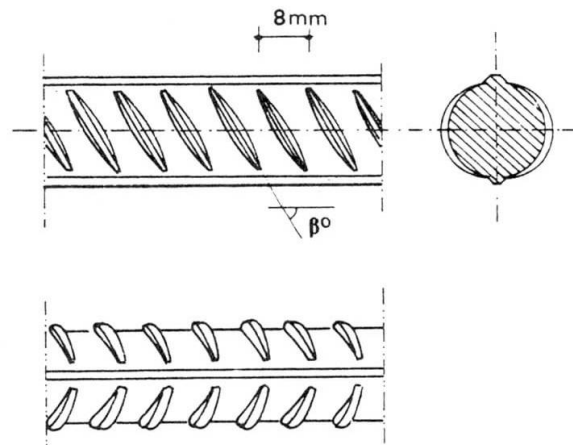
Fig. 2-a Geometrical characteristics of the deformed bar used in the tests

guide rings for the special provisional sleeves

deformed bar with two ribs

original bar after machining

special provisional sleeve coated with paraffin
to facilitate extraction before testing
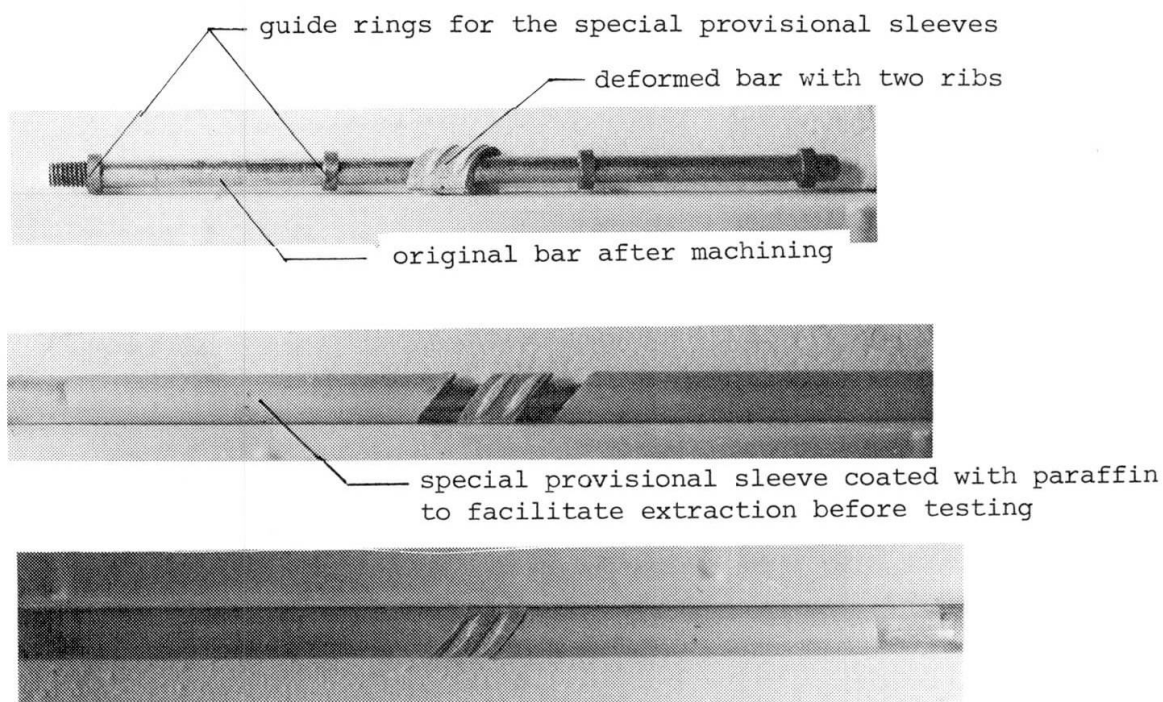
external aspect of the test bar before concrete casting, with the
provisional sleeves closed up to the ribbed element

Fig.2-b - The two-ribbed element of deformed bar and the special provisional
sleeves
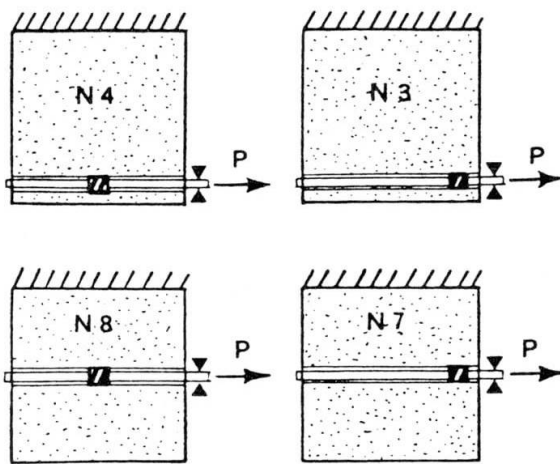
Fig. 3-a - Longitudinal cross-
          sections of the test
          specimens to show
          the position of the
          bar
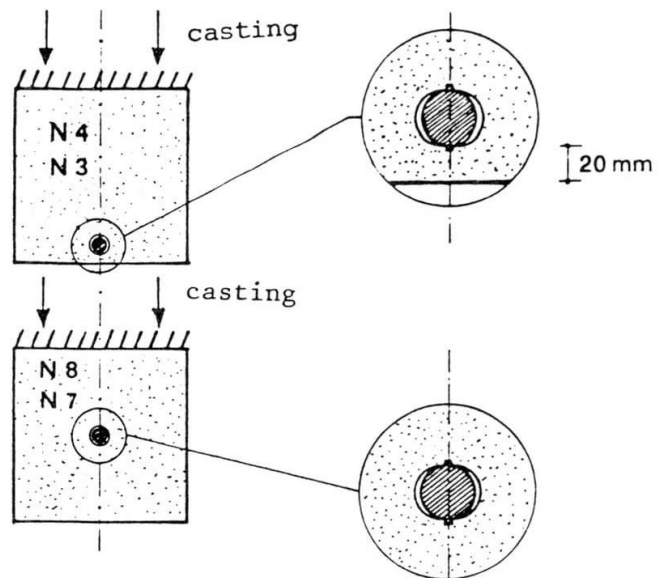
Fig. 3-b - Transversal cross-
          sections of the test
          specimens and orien-
          tation of the lugs
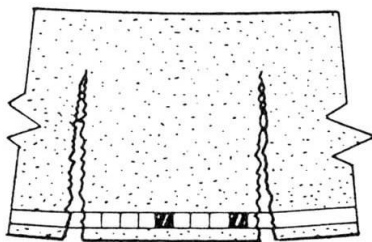
Fig. 3-c - Actual situation of
          a beam in bending:
          the test specimens
          N3 and N4 simulate
          this situation
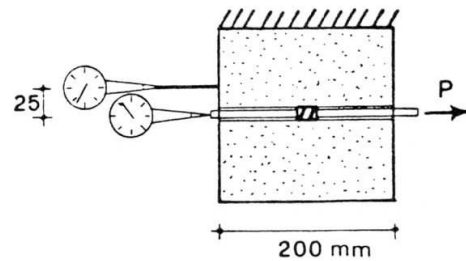
Fig. 3-d - Instruments to
          measure slip
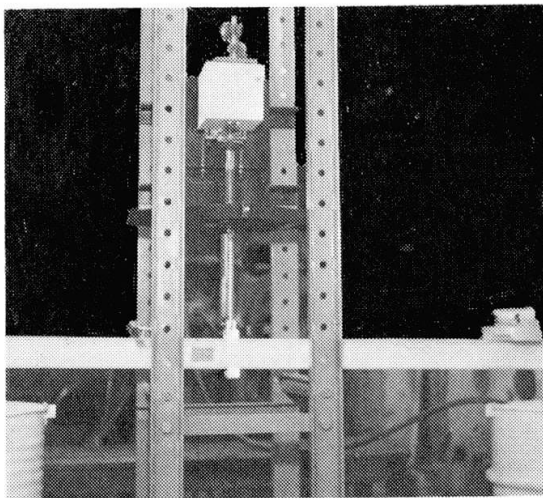
Fig. 4 , 5 - View of the loading set-up: the loads
            are applied via watertanks and levers,
            which makes the load reversal possible
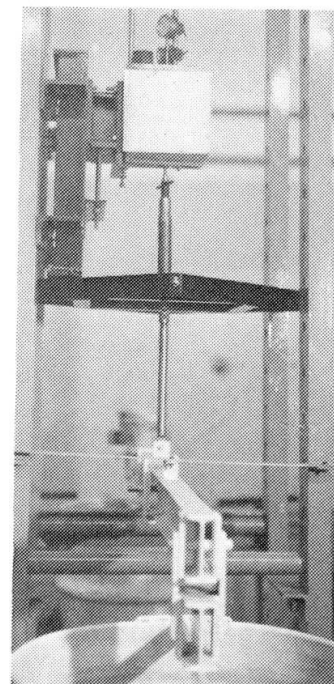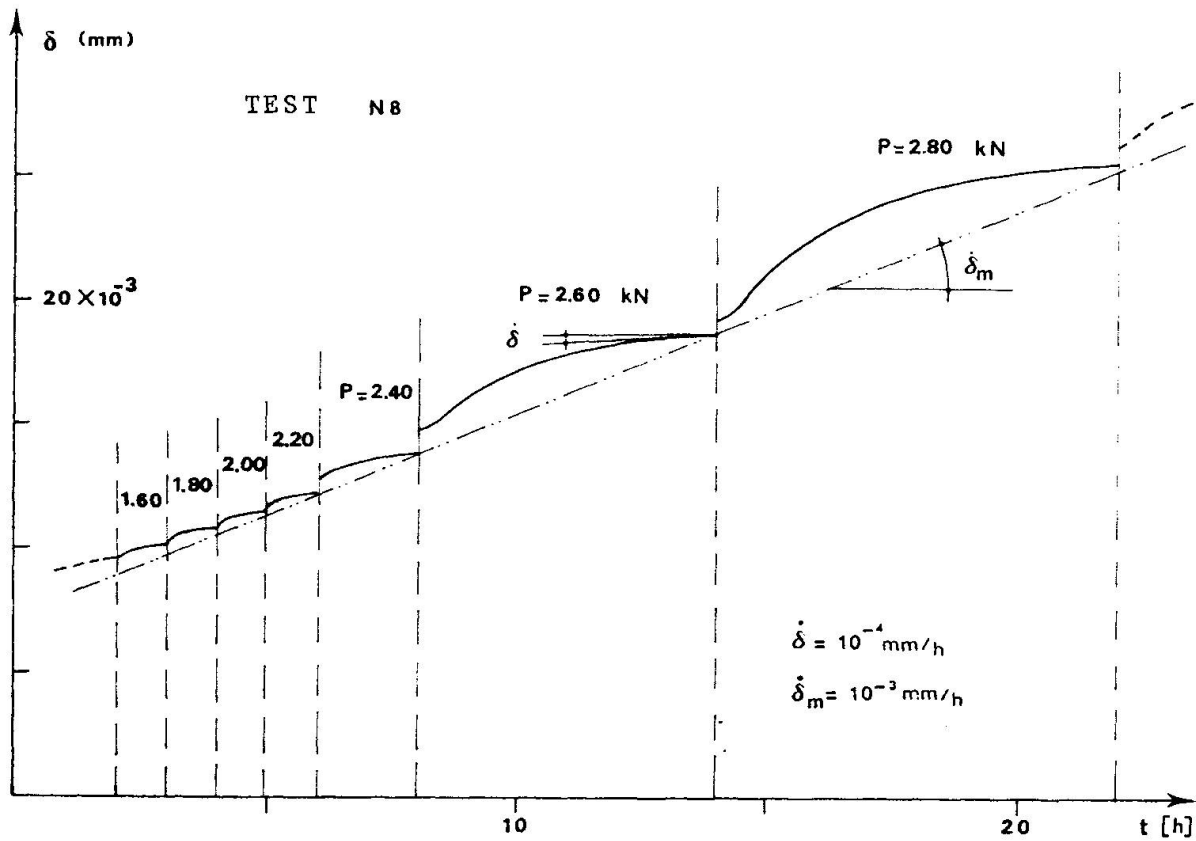
Fig. 6 - Slip curve for different load steps, versus time
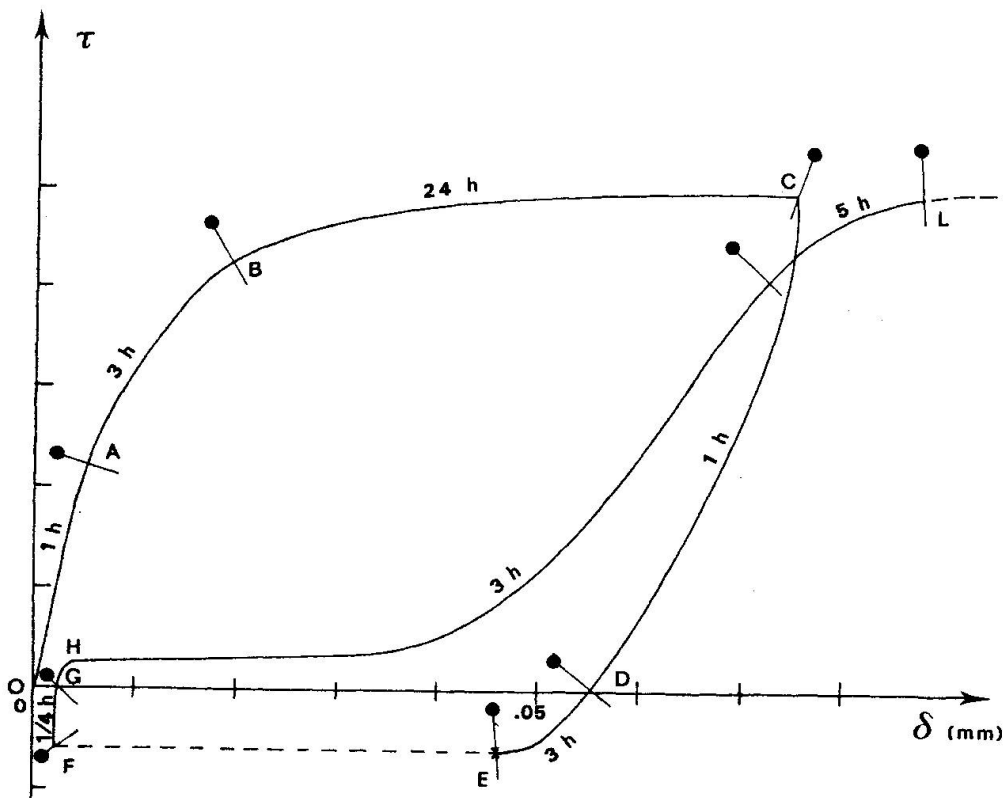
Fig. 7 - Bond-slip curve with the length of time taken by the various phases

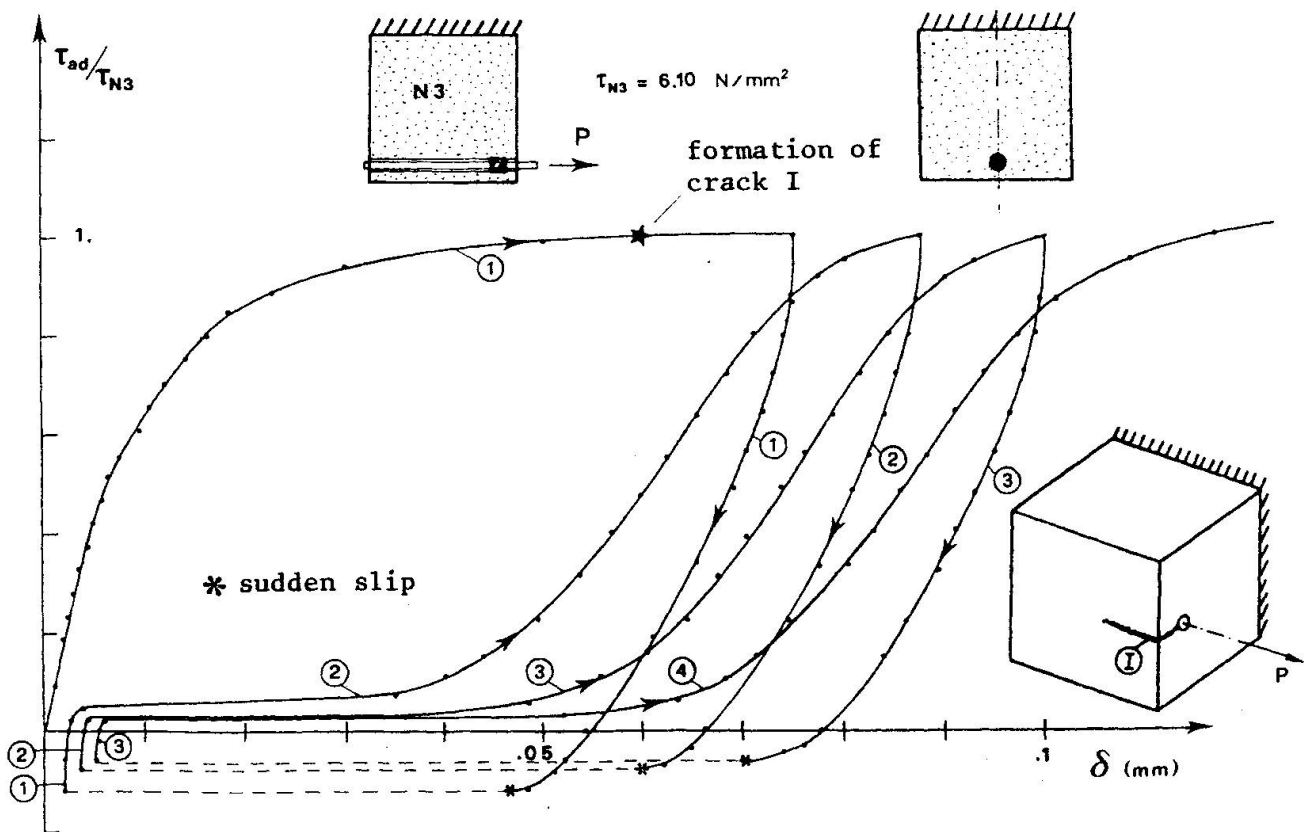Fig. 8 - Bond-slip curves with cyclic loading (the maximum bond stress is kept constant in each cycle)

Fig. 9 - Bond-slip curves with cyclic loading (the maximum bond stress is kept constant in each cycle)
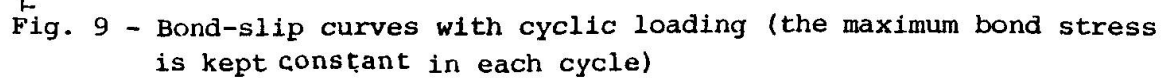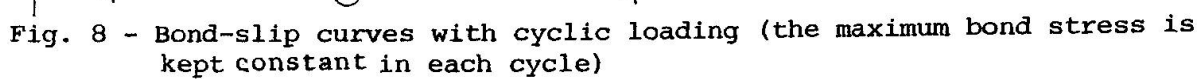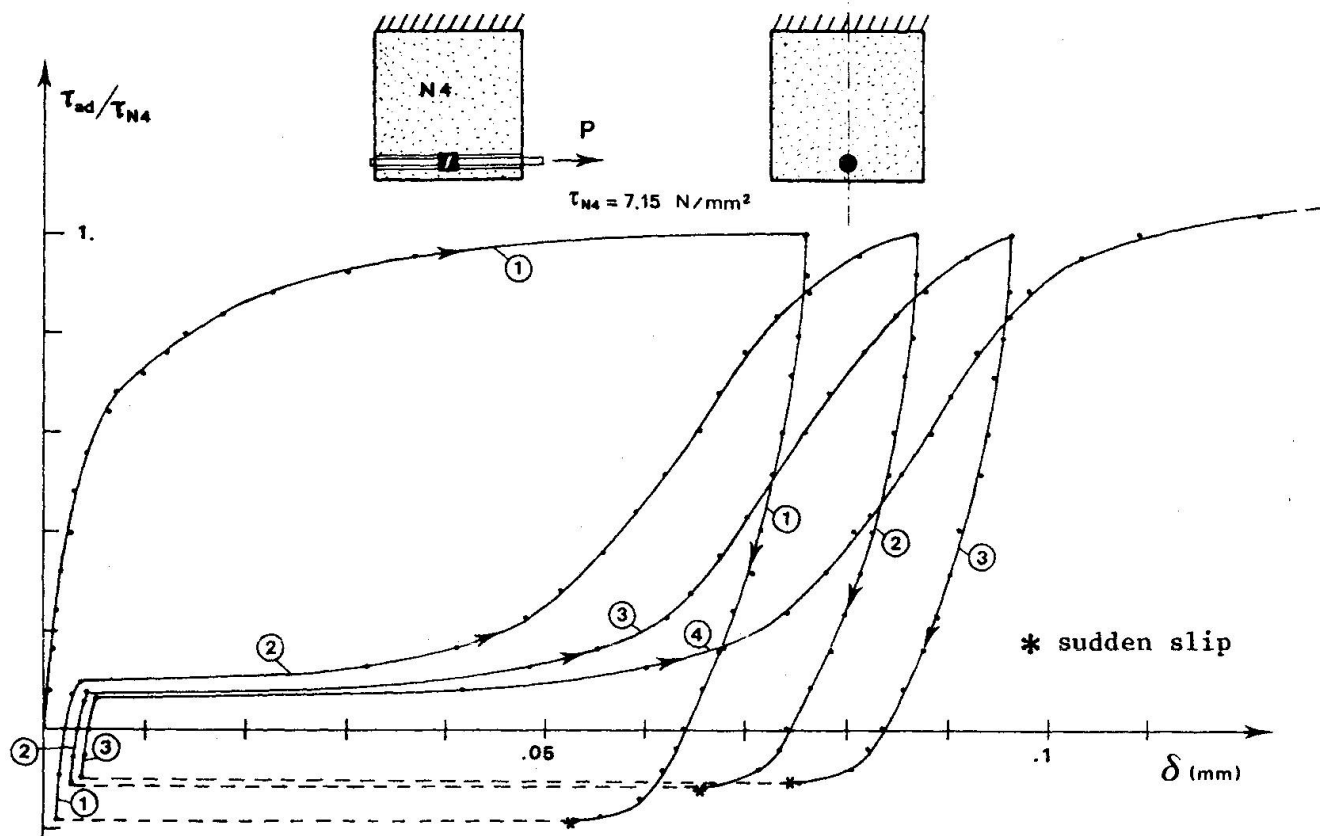
Fig. 10 - Bond-slip curves with cyclic loading (the maximum bond stress is
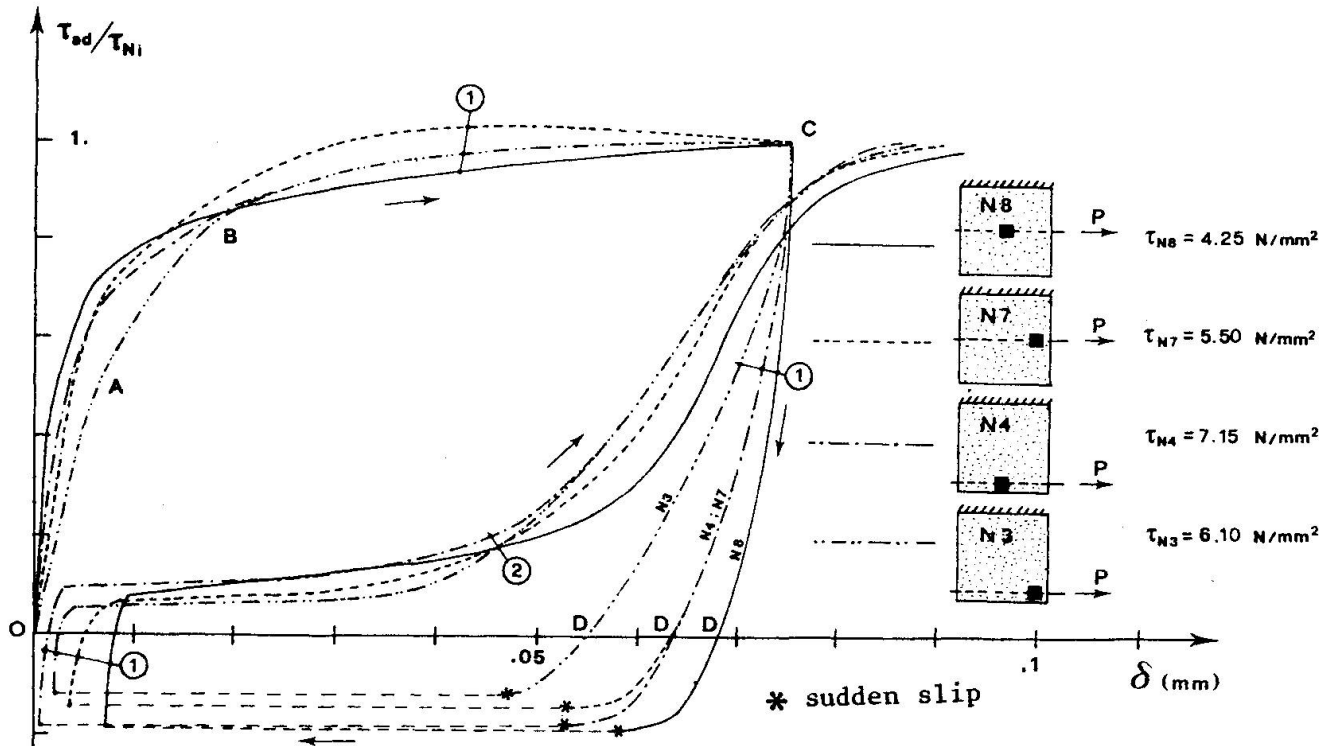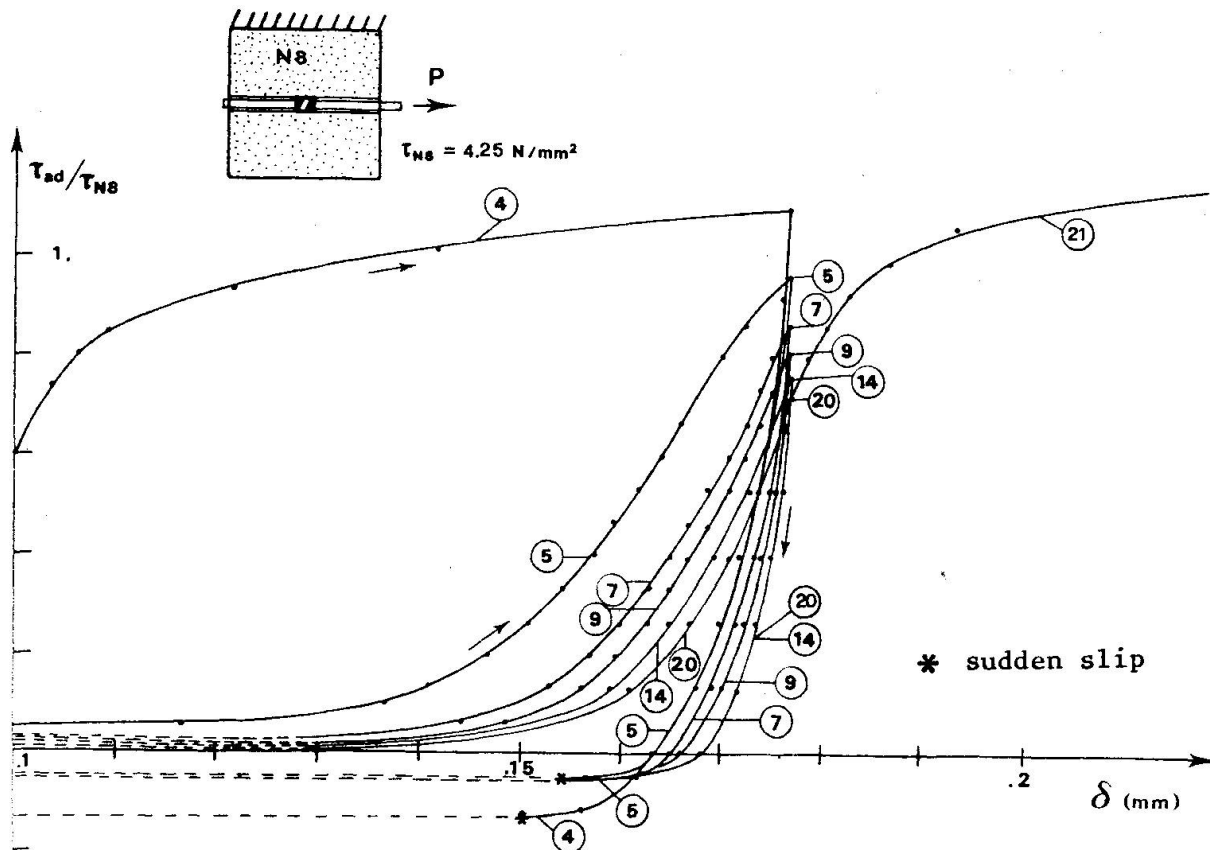   kept constant in each cycle).

Fig. 11 - Bond-slip curves with cyclic loading (the maximum bond stress is
         kept constant in each cycle)

Fig. 12 - Bond-slip test curves, with the bond stress related to the nominal stress τ_{Ni} of each test specimen

Fig. 13 - Bond-slip curves with cyclic loading (the maximum slip is kept constant in each cycle)
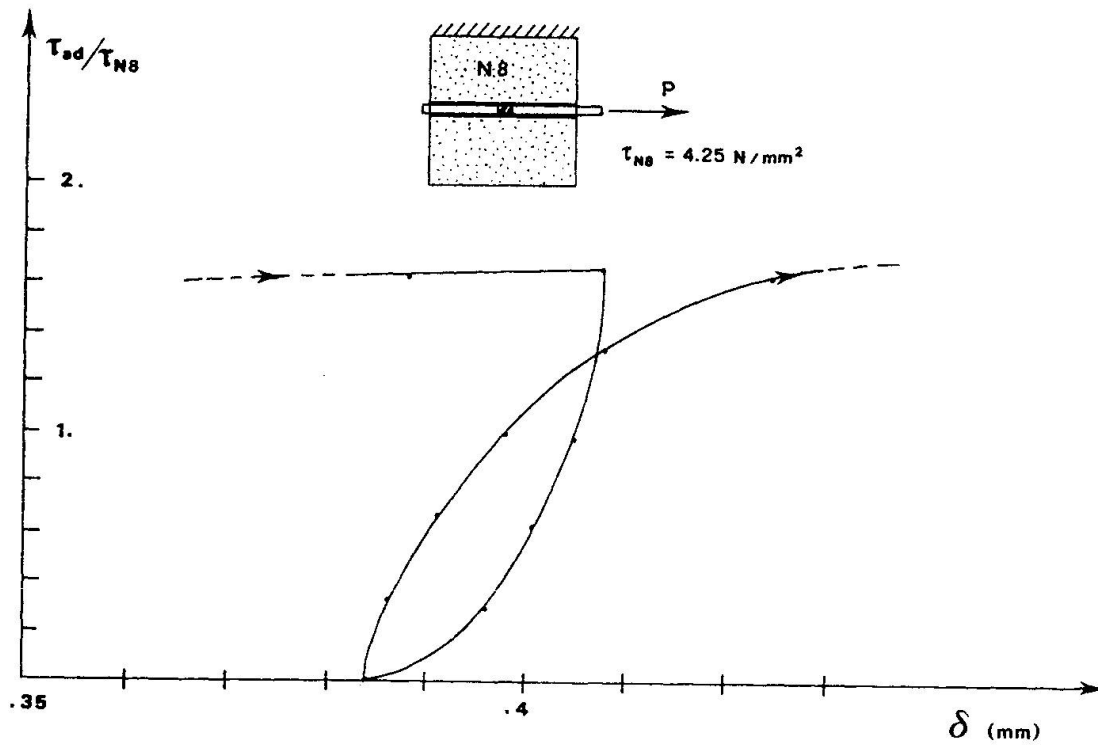
Fig. 14 - Bond-slip curve obtained by reducing the load to zero and re-loading
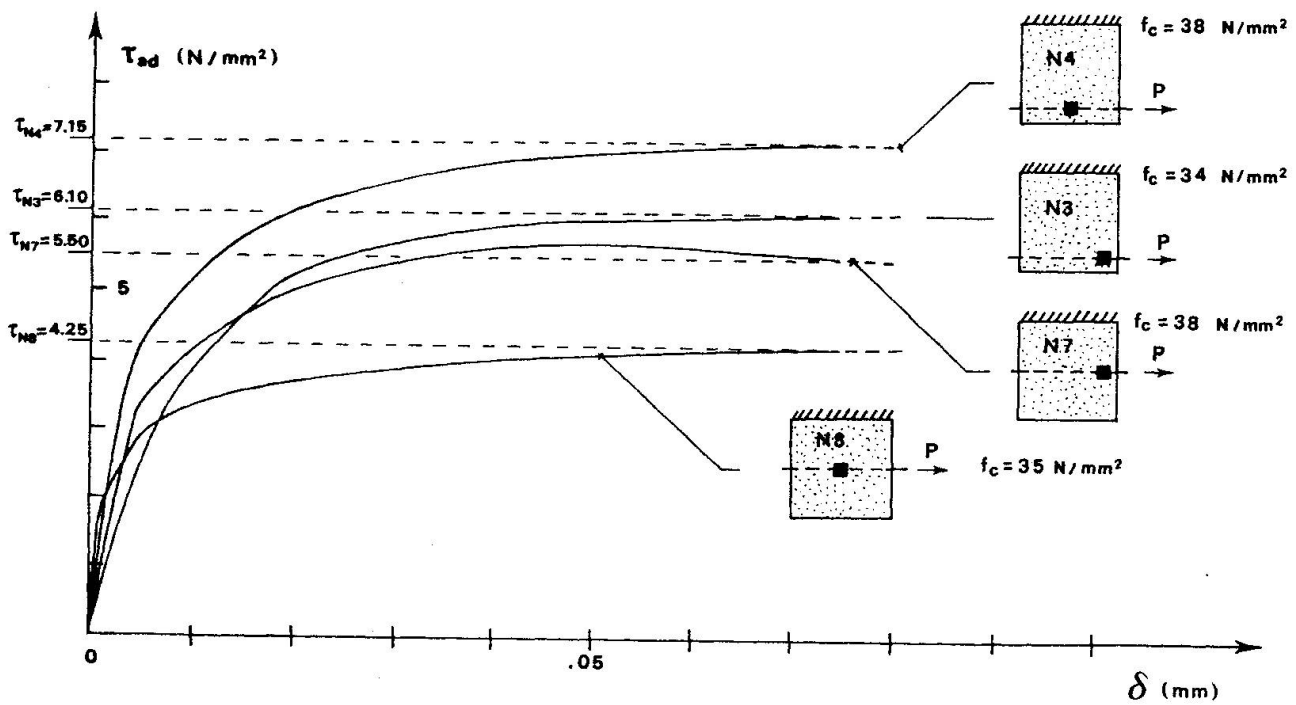   without sign reversal

Fig. 15 - Comparison between bond-slip curves for monotonically increasing load
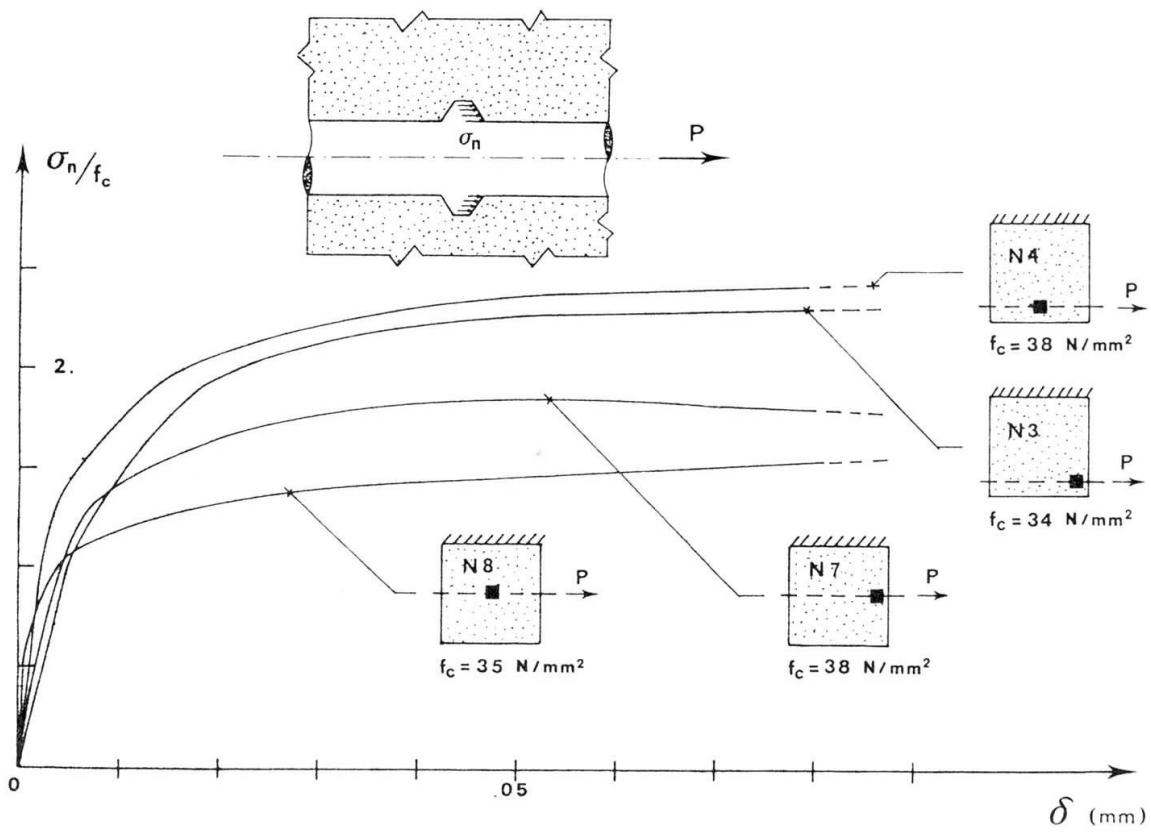
Fig. 16 - Bearing stress on the concrete related to the prismatic strength
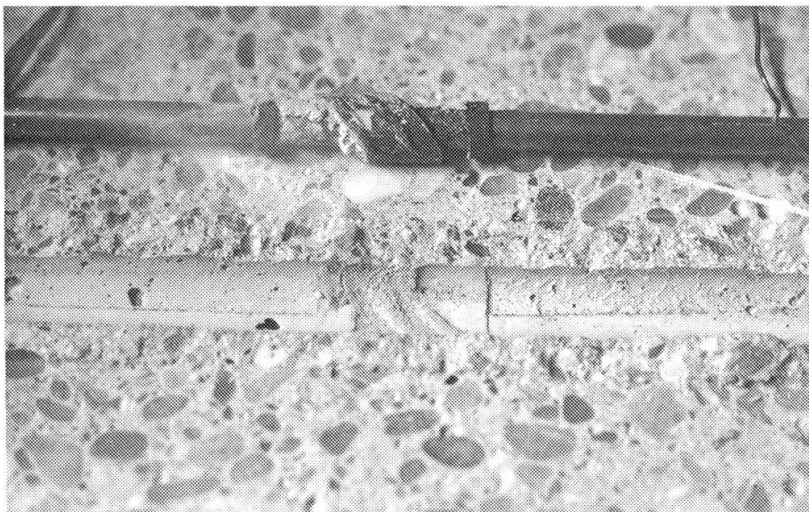of each test specimen

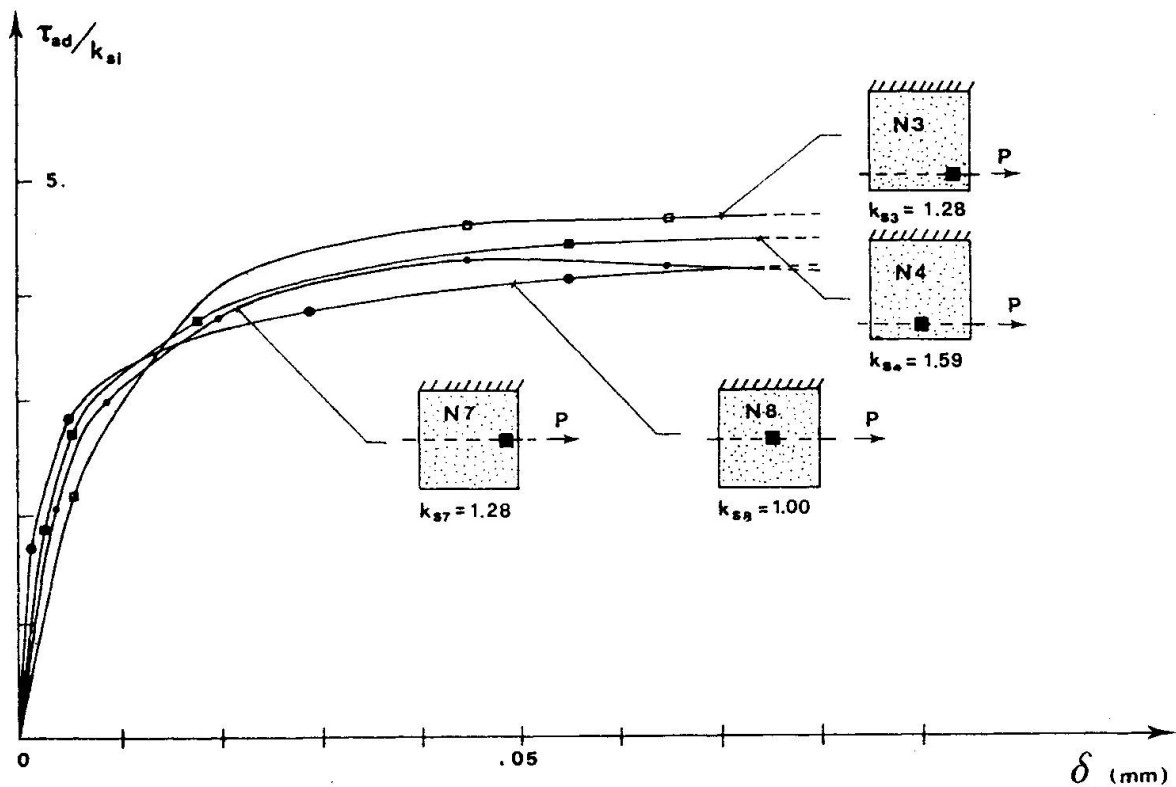Fig. 17 - Detail of the groove left by the bar

Fig. 18 - Bond-slip curves, with the bond stress divided by the hardness
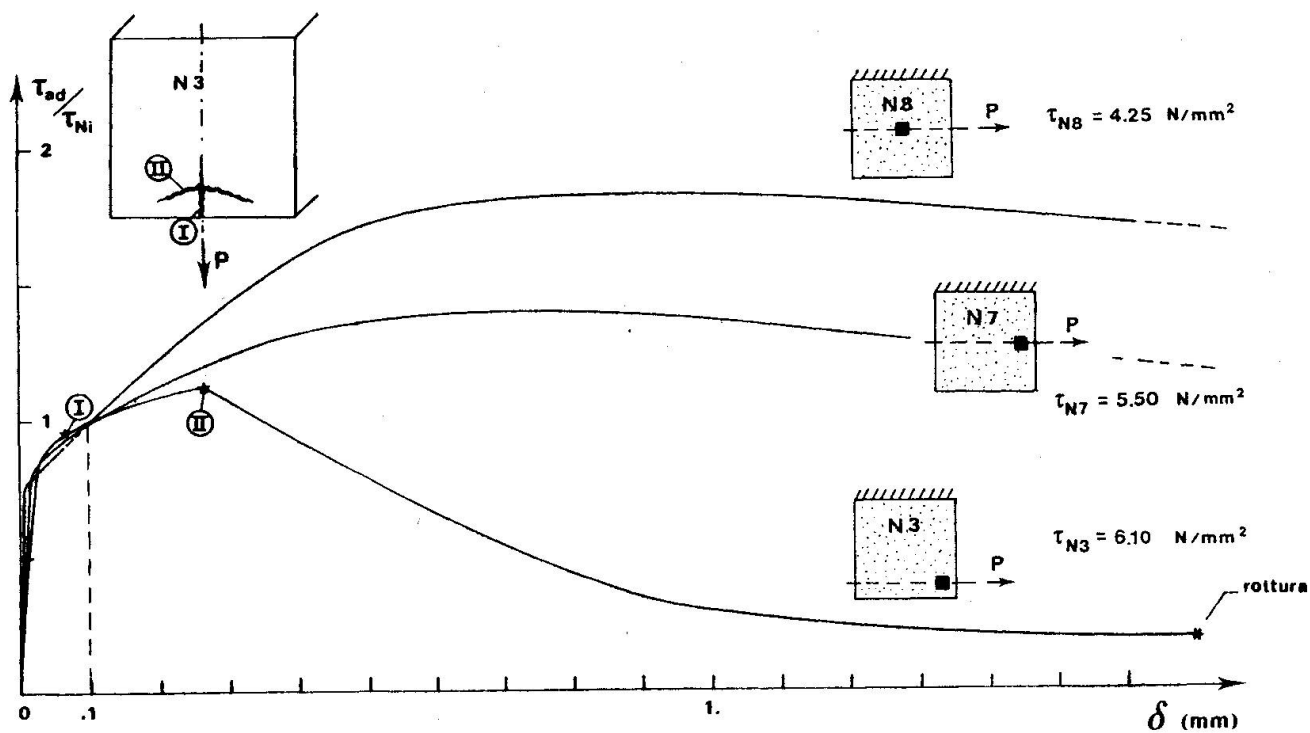   index, for the different specimens

Fig. 19-a - Bond-slip curves for large displacements

Fig. 19-b-Cracking of test specimen N3 at the end of the test. A large transversal crack can be seen on the front face as well as a split
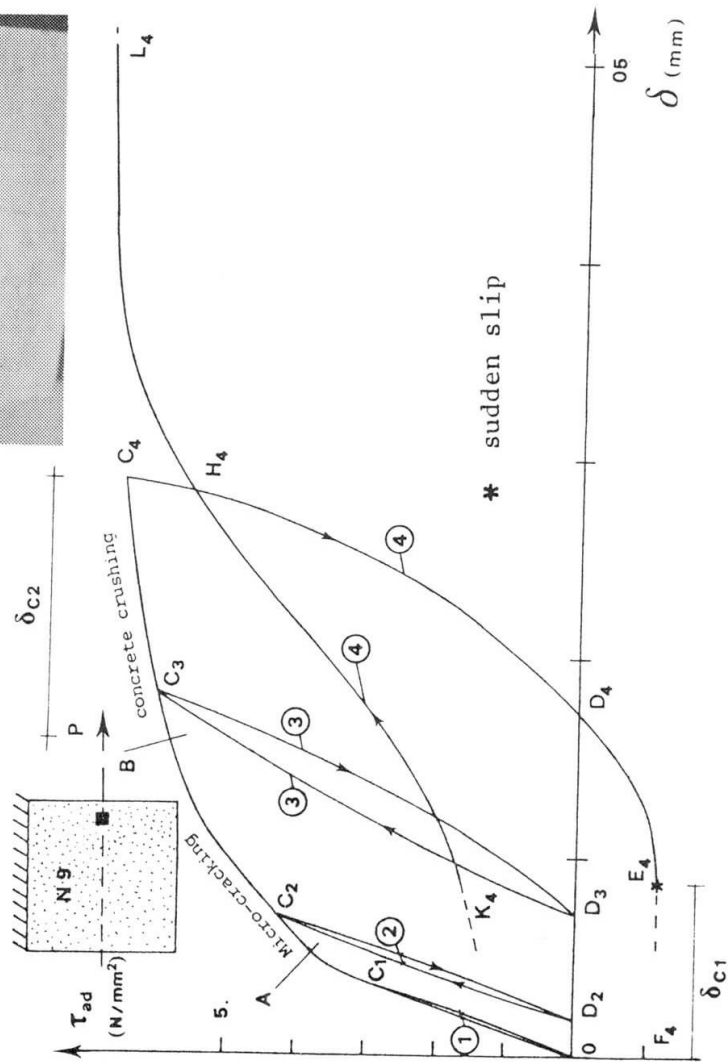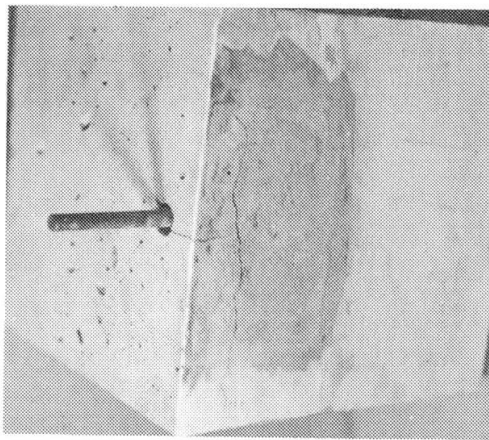
a) Monotonically increasing loads (branch AB C₄ Fig. 20)

b)

crushing

c) Unloading branch (C₄D₄): situation with no load applied (point D₄)

d) situation for loading of opposite sign (D₄E₄)

e)

f) Reloading (branch O K₄ H₄ L₄)

Fig. 21 - Micro-cracking mechanism

nominal failure surface

Fig. 20 - Load cycles in the elastic phase and at the beginning of the permanent displacement phase

τ_{ad} (N/mm²)

concrete crushing

Micro-cracking

* sudden slip

δ (mm)

	N8	N7	N4	N3
Prismatic strength at the load rate 1.5 N/mm²/sec. (+)	$f_c = 35$	$f_c = 38$	$f_c = 38$	$f_c = 34$
Curing period at start of test (in days)	90	80	70	60
Nominal hardness (+) of the concrete layer around the bar (**)	10.5	13.5	16.7	13.5
Index of hardness K_{si}	1	1.28	1.59	1.28
Nominal hardness of the outer layer of the specimen (+)	16.5	20.7	22.5	22.8

Table II - Mechanical characteristics of the concrete

(+)   Measured after 150 days of curing

(**) The hardness was measured by sclerometric tests, averaging 20 readings. A special reduced prod was fitted to a Schmidt sclerometer to reach the concrete groove formed by the bar after having cut the test specimen and removed the bar.
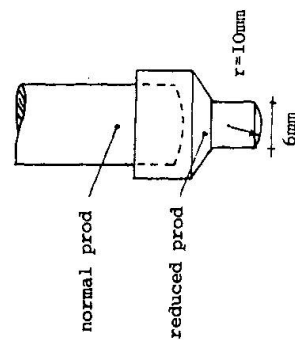
The normal prod for plane surfaces gave values 1,3 times higher than with the smaller prod.

normal prod

reduced prod

r=10mm
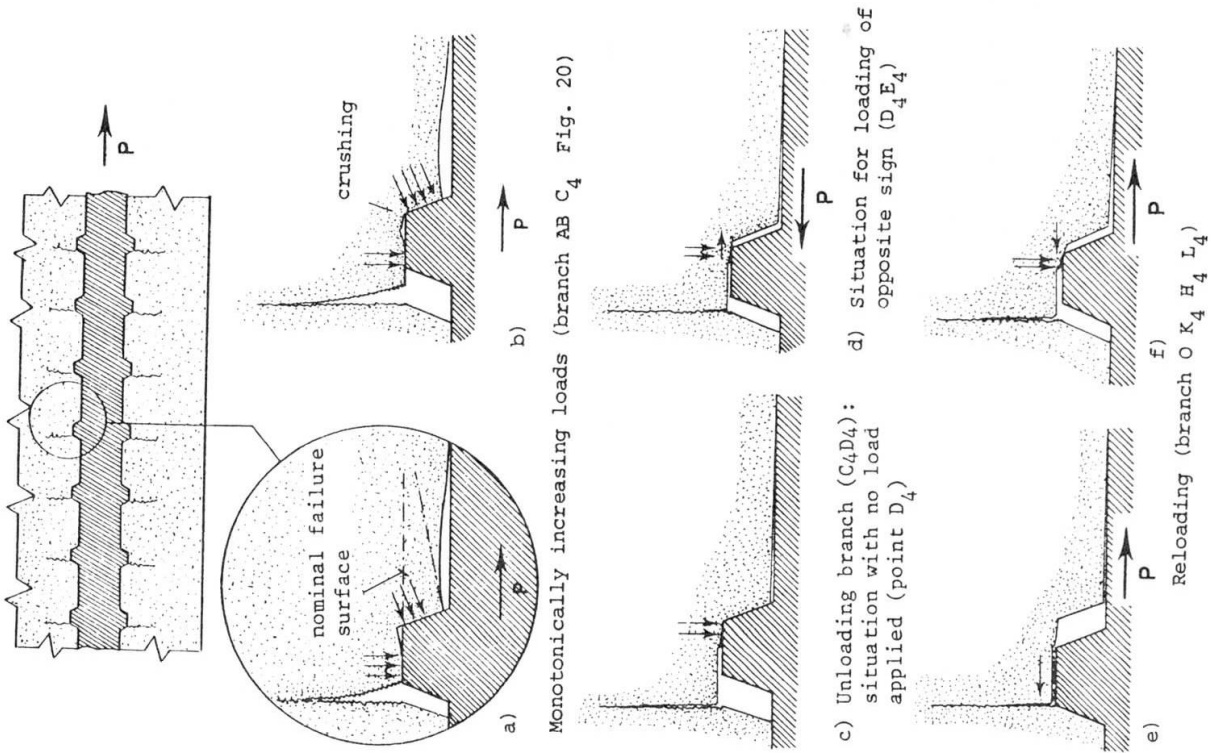
6mm

Concrete MIX

- Portland Cement (compressive strength = 41.4 N/mm²)
  nominal cement quantity 3 KN/m³
  actual cement quantity 3,32 KN/m³

- water-cement ratio: A/C = .65

- aggregate graduation and size

maximum size (mm)	15-7	7-3	3-1	1-0,5	0,5-0,2	0,2-.075	.075 -0
percentage %	34.1	25.1	20.7	8.3	7.6	3.7	.5

The aggregate are open quarry, natural aggregates.

Casting

- Expanded polystyrene molds for the test specimens (cubes)
- compaction by table vibrator (50 Hz) for 5+5 seconds
- slump: specimens N3 and N4 (1st casting), slump = 5.5 cm
  specimens N7 and N8 (2nd casting), slump = 6.0 cm

Mechanical Characteristics of concrete

- Average cylindrical strength: $f = 36.5$ N/mm² measured on three cylinders with load rate 1.5 (N/mm²)/sec.

- elastic modulus: $E_o = 26500$ N/mm² measured with load rate 0.015 (N/mm²)/sec.

- tensile strength 3.08 N/mm² (measured) on a cylinder (D = 10 cm; l = 30 mm) with load rate 1.5 (N/mm²)/sec.

Table I